How to cite: *Angew. Chem. Int. Ed.* **2022,** *61,* e202116217
International Edition: doi.org/10.1002/anie.202116217
German Edition: doi.org/10.1002/ange.202116217

Neurochemistry

Simultaneous Counting of Molecules in the Halo and Dense-Core of Nanovesicles by Regulating Dynamics of Vesicle Opening

*Xiulan He and Andrew G. Ewing**

Abstract: We report the discovery that in the presence of chaotropic anions (SCN^-) the opening of nanometer biological vesicles at an electrified interface often becomes a two-step process (around 30 % doublet peaks). We have then used this to independently count molecules in each subvesicular compartment, the halo and protein dense-core, and the fraction of catecholamine binding to the dense-core is 68 %. Moreover, we differentiated two distinct populations of large dense-core vesicles (LDCVs) and quantified their content, which might correspond to immature (43 %) and mature (30 %) LDCVs, to reveal differences in their biogenesis. We speculate this is caused by an increase in the electrostatic attraction between protonated catecholamine and the negatively charged dense-core following adsorption of SCN^-.

Secretory vesicles have been implicated in a variety of physiological[1–3] and pathological process,[4–7] which involve triggered exocytosis and extensively investigated in several cell types.[8–10] There are two main types of secretory vesicles including small synaptic vesicles and large dense-core vesicles (LDCVs).[11] LDCVs are key organelles for secretion of hormones and neuropeptides, and contain two compartments, the halo and the dense-core.[11–13] Due to their complexity of constituents and structure, several approaches have been applied to study them. These include transmission electron microscopy,[14] dynamic light scattering,[15] nanoparticle tracking analysis,[16] nanopore resistive pulse methods,[17–19] neurotransmitter quantification by electrochemical cytometry[20] (e.g., vesicle impact electrochemical cytometry (VIEC),[21,22] and intracellular VIEC,[23]) and nanoscale secondary ion mass spectrometry.[24,25] The VIEC process involves a biological vesicle adsorbing on an electrified interface and opening a pore in the vesicular membrane via electroporation followed by oxidation of molecules in the interior.

Recently, our group correlated molecule count and release kinetics with vesicular size by use of an open carbon nanopipette,[26] and quantified the nanovesicle size and catecholamine content simultaneously by resistive pulses in nanopores and VIEC.[27] However, to the best of our knowledge, the simultaneous counting of molecules in the native halo and dense-core of nanovesicles, which benefits the deeper understanding of the biogenesis and function of LDCVs, has not yet been accomplished. To realize simultaneous counting from the two nanoscopic compartments, the critical step is to slow down the diffusion of catecholamine molecules from the dense-core to the halo. Recently, we discovered that the exocytosis process can be slowed down by introducing a chaotropic effect between membrane lipids and chaotropic counteranions placed in the stimulation solution,[28] suggesting the chemical interaction is an enabling approach to quantitatively discriminate the content of the intravesicular compartments.

Herein, we simultaneously discriminated the content of the halo and dense-core of individual chromaffin vesicles by regulating the dynamics of vesicle opening in VIEC (see Supporting Information S1). A carbon-fiber disk microelectrode was placed in a homogenizing buffer solution of vesicles including different counteranions (e.g., Cl^-, Br^-, NO_3^-, ClO_4^-, and SCN^-), and a potential of +700 mV was applied to record the current spikes resulting from vesicle opening. Examples of VIEC amperometric traces obtained are shown in Figure S1. Each current transient corresponds to a single vesicle opening event. When the counteranion in the vesicle analysis solution is SCN^-, the frequency of vesicle opening events is significantly higher than that obtained with other counteranions (Figure S2, p values are listed in Table S1). This difference can be attributed to stronger adsorption of vesicles on the electrode surface and/or a higher possibility of vesicles opening leading to current spikes.

Interestingly, in contrast to release peaks normally observed in 10 mM KCl, when we examined vesicles in 10 mM KSCN, numerous doublet spikes were observed (30 % of all events). To exclude the possibility of two overlapping current spikes, we performed the VIEC experiment in a diluted solution of vesicles with 10 mM KSCN (Figure 1A). Among 41 recorded spikes in a 10-min amperometric trace, 14 doublets were observed (Figure S3). This suggests that the doublets are from the oxidization of catecholamine located in the halo and dense-core. A normal single-peak spike is shown in Figure 1B for comparison. The

[*] Dr. X. He, Prof. A. G. Ewing
Department of Chemistry and Molecular Biology, University of Gothenburg
Kemivägen 10, 41296 Gothenburg (Sweden)
E-mail: andrew.ewing@chem.gu.se

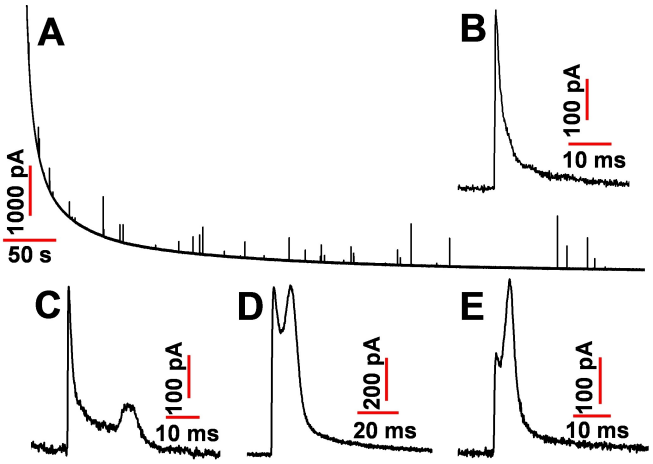

Figure 1. A) A typical VIEC trace obtained from chromaffin vesicles in 10 mM KSCN. B) A normal single-peak current spike. C), D), and E) Three types of doublet spikes obtained from (A).

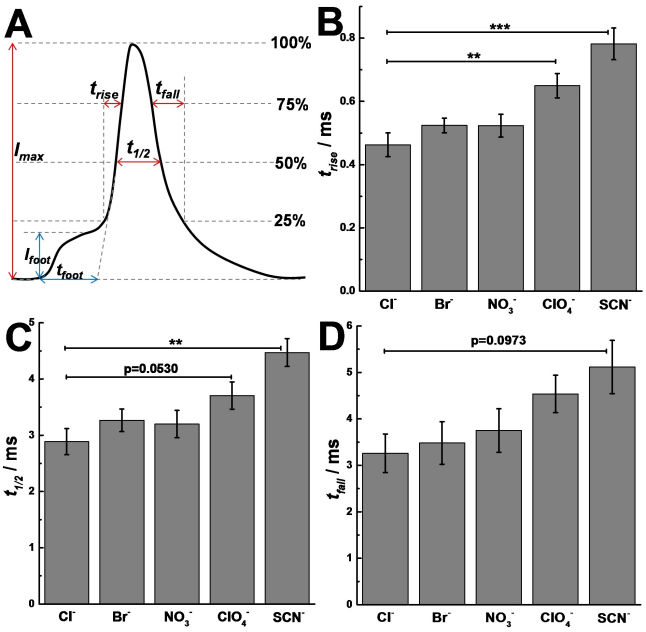

Figure 2. A) Scheme of different parameters used for the spike analysis. B), C), and D) Comparisons of t_{rise}, $t_{1/2}$, and t_{fall} from VIEC with chromaffin vesicles in 10 mM K^+ solution including different counter-anions (e.g., Cl^-, Br^-, NO_3^-, ClO_4^-, and SCN^-). Pairs of data sets were compared with a two-tailed Mann–Whitney rank-sum test; ***, $p < 0.001$; **, $p < 0.01$; *, $p < 0.05$.

doublets obtained in the presence of SCN^- can be divided into three types based on the maximum amplitude of the current (I_{max}) for the two peaks (Figure 1C–E). We assume these different types of doublets are related to the size of the protein dense-core and its catecholamine content in individual vesicles.

To determine if the doublets in the presence of KSCN are indeed from the same vesicle, we compared the number of molecules oxidized in individual spikes in the presence of different counteranions. The number of molecules oxidized in individual spikes can be quantified via the Faraday equation. We found that the mean number of molecules oxidized for each current spike in 10 mM K^+ was not significantly changed with different counteranions (Figure S4, p values are listed in Table S2). Moreover, considering the possible leakage during vesicle preparation, the number of molecules obtained by VIEC is consistent with the result measured by intracellular VIEC (Figure S5). This demonstrates the doublet spikes are from oxidation of single vesicles, which might correspond to the oxidation of halo (1st peak) and dense-core content (2nd peak).

To further understand the formation of doublets, we compared other parameters (Figure 2A) for global current spikes obtained from vesicles opening in 10 mM K^+ with different counteranions. We evaluated the 25–75 % peak rise time, t_{rise}, the peak half width, $t_{1/2}$, and the 75–25 % peak fall time, t_{fall}. The medians of peak parameters for the main peak are summarized and compared in Figure 2B–D. A significant increase in the value of t_{rise}, and $t_{1/2}$ is observed with chaotropic counteranions (e.g, SCN^-) (p values are listed in Tables S3, S4), compared with the counteranions of kosmotropes (e.g., Cl^-). However, the value of t_{fall} does not show a statistically significant change while trending upward (p values are listed in Tables S5). Thus, the opening and collapse of the vesicular membrane pore after electroporation in the presence of chaotropes has been decelerated. In contrast, a decrease in I_{max} is observed (Figure S6, p values are listed in Tables S6) when vesicles are analyzed with the counteranion changed from kosmotropes (e.g., Cl^-) to a chaotrope (e.g., SCN^-). This suggests that the opening pore during vesicle opening is smaller for the chaotropic counteranions. These results suggest that the ionic specificity, or the chaotropic effects, drive the different dynamics of vesicle opening and thereby induce the formation of doublet spikes.

When a pore opens in a vesicle in normal buffer solution (Cl^-), the falling part of the resulting spike can be fitted by either a single (Exp) or double exponential (Dblexp) decay, which correspond to the opening of vesicles without a dense-core (NDCVs) and LDCVs, respectively.[27,29,30] To investigate the effects of anionic species on the opening of LDCVs, we summarized and compared the fraction of Dblexp spikes for different counteranions (Figure S7). The fraction of Dblexp spikes decreases when the counteranions are changed from kosmotropes (73 % for Cl^-) to chaotropes (43 % for SCN^-) (p values are listed in Table S7). This suggests that the dynamics of LDCV opening can be regulated by the counteranion species, which is consistent with the effects on the falling time. The fraction of Dblexp spikes for vesicles in Cl^- solution reveals that the fraction of NDCVs is around 27 %, with 73 % LDCVs. For SCN^- counteranions, doublets are observed for 30 % of events. The remaining 43 % percent of LDCVs represent events where the molecules in the halo and dense-core are not counted simultaneously. It has been demonstrated that there are two populations of LDCVs in chromaffin cells.[31,32] It appears that these three results (27 % Exp, 30 % doublet, and 43 % other spikes) belong to three different vesicle opening mechanisms (NDCVs, mature LDCVs, and imma-

ture LDCVs, respectively). To better understand their difference, we log-normalized frequency histograms to describe the distribution of the number of molecules for Exp, Dblexp, and doublet spikes. As shown in Figure S8, the number of molecules for Dblexp spikes is larger than that for Exp spikes, but smaller than that for doublet spikes. This supports our hypothesis that the NDCVs load the least catecholamine, while the mature LDCVs load the most molecules.

To further understand the mechanism, we used six different concentrations of SCN^- from 0 to 10 mM (with corresponding concentrations of Cl^- of 10 to 0 mM, respectively) in 10 mM K^+ solution to carry out the VIEC experiments. We calculated and summarized the ratio of $N_{Dblpeak}/N_{Dblexp}$ (i.e., the number of doublets vs. the number of Dblexp spikes) for different SCN^- concentrations, and found the ratio increases linearly with KSCN concentration (Figure S9, p values are listed in Table S8).

To explain the formation of doublets, we propose a two-step opening mechanism (Figure 3), where the adsorption of chaotropic anions and the pH gradient play an important role. The biogenesis of LDCVs involves the budding of immature LDCVs (pH 6.3–5.7) from the trans-Golgi network (pH 6.5–6.2) followed by several maturation steps to form mature LDCVs (pH 5.5–5.0).[33–35] During these steps, the acidic proteins of the dense-core including chromogranin A, B, secretogranin II–IV are folded, protonated catecholamines (e.g., epinephrine,[36] $pK_a = 8.55$; norepinephrine,[37] $pK_a = 8.4$), and other molecules or ions (e.g., ATP and Ca^{2+})[38] are loaded and bound to the dense-core by electrostatic forces.[39,40] It has been demonstrated that the kosmotropes stabilize folded proteins and lipid bilayers via salting-out, whereas chaotropic ions destabilize them via salting-in, and change their structures or even reverse their charge.[41–44] For kosmotropes (e.g., Cl^-), no change occurs on the structure and charge of the vesicle membrane and dense-core. The LDCVs open in one-step resulting in single-peak spikes with double-exponential decays; catecholamines rapidly diffuse from the dense-core to the vesicular halo. In contrast, the chaotropes (i.e., SCN^-) prefer to adsorb on lipids and proteins resulting in a looser vesicle membrane and more negatively charged dense-core. In addition, it is possible that the chaotropes interact with the catecholamines, and one or the other of these processes leads to a higher ionic attractive energy between the bound catecholamine and dense-core after adsorption of SCN^-. This restricts the diffusion of catecholamine from the dense-core to halo during the initial vesicle opening, and the halo content oxidizes in the first step. Moreover, the adsorbed SCN^- decreases the hydration around the dense-core[45] that also restricts diffusion of catecholamines from the core to the halo. Following vesicle opening, we suggest the increasing intracystic pH partially deprotonates the catecholamine molecules, leading to a smaller electrostatic attraction. Thus, the catecholamines bound to the dense-core are oxidized in the second step. Compared to the mature LDCVs, the immature LDCVs have a looser dense-core structure thus loading fewer catecholamine molecules, and a smaller pH gradient (intracystic vs. extracystic), which impedes the occurrence of two-step opening.

We used the chaotrope-induced doublet peaks to simultaneously count catecholamine molecules in the nanoscopic vesicular halo and dense core (Figure 4A). We analyzed 284 pairs of peaks. The number of molecules for the 1st peak of the doublets was tightly correlated with the number of molecules for the paired 2nd peak (Figure 4B). This can be

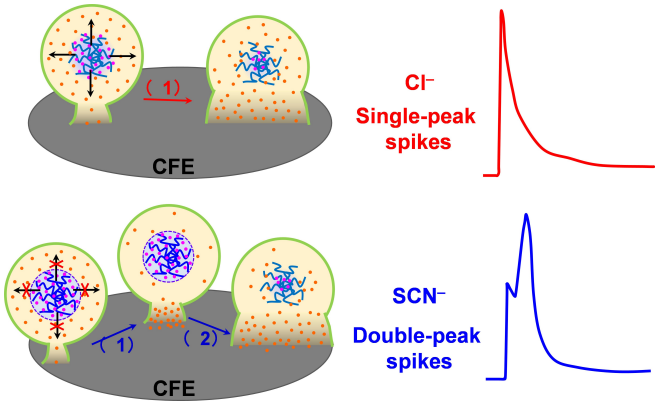

Figure 3. Illustration of a proposed two-step opening mechanism induced by SCN^-. The effects of chaotropes (SCN^-) on the lipid bilayer induce a smaller opening, and SCN^- adsorbed to the dense-core offers a stronger electrostatic attraction to help the binding of catecholamine. This leads to slower diffusion, resulting in a two-step oxidation of catecholamine in the halo and dense-core.

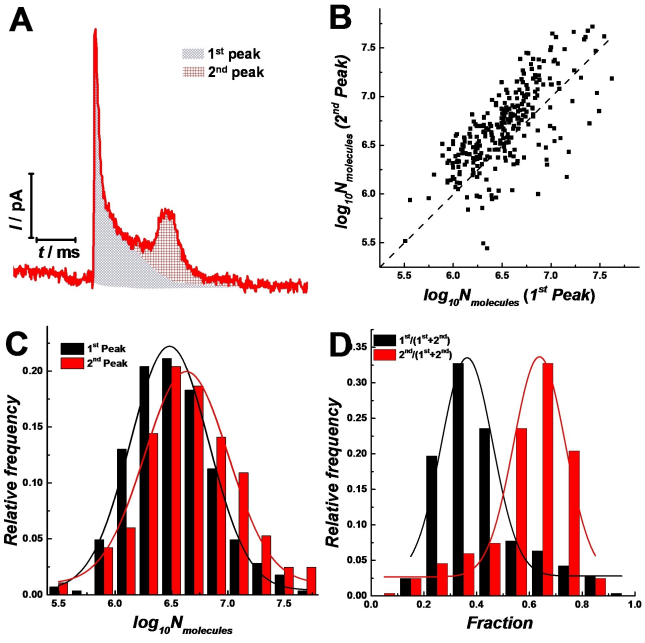

Figure 4. A) Scheme to count and compare molecules in the 1st and 2nd peak of doublet spikes, corresponding to the vesicular halo and dense-core, respectively. B) Relationship between the paired 1st peak content vs. 2nd peak content. C) Log-normalized frequency histograms of 1st and 2nd peak content which is fitted by Gaussian, respectively. D) Normalized frequency histograms of the fraction of the total content in the 1st (halo) and 2nd (dense core) peak. These are shown with best Gaussian fits.

explained by the different states of catecholamine in the halo (freely dissolved) and dense-core (bound) which can be correlated and regulated by the osmotic pressure in vesicles. Moreover, histograms of the number of molecules and fractions released from the halo and dense-core are shown in Figure 4C, D, respectively. The distribution of the number of molecules obtained from the 1st and 2nd peak (Figure 4C) is fitted by Gaussian, which is consistent with the distribution of the number of molecules obtained from normal single-peak spikes.[21,22] The medians of fractions for the halo and dense-core content (Figure 4D) are 38 % and 62 %, respectively. Because of the asymmetrical distributions, we further normalized the frequency of central part (Figure S10). The maximum fractions for molecular count in the halo and dense-core are 32 % and 68 %, respectively. This is the first direct measurement of the fraction of content in the halo and dense core for mature LDCVs, which offers a quantitative index to investigate the effects of chemicals or drugs on individual vesicular compartments.

In conclusion, we present the discovery that doublet spikes induced by chaotropes (SCN^-) are recorded from nanometer chromaffin vesicles opening when a vesicle opens on an electrified interface. Furthermore, the 1st and 2nd peaks correspond to the oxidization of molecules from the halo and dense core, respectively, allowing us to obtain a molecular count independently in these two nanoscopic compartments. Moreover, the vesicles can be classified into three groups including NDCVs, immature LDCVs, and mature LDCVs. A stronger electrostatic interaction and a higher pH gradient play a dominant role in observation of the doublets resulting from the opening of mature LDCVs. These observations should be helpful for understanding the biogenesis of LDCVs, effects of chemicals on vesicular compartments, mechanisms of neural plasticity, and neurodegenerative diseases.

Acknowledgements

The European Research Council (ERC Advanced Grant Project No 787534 NanoBioNext), Knut and Alice Wallenberg Foundation, and the Swedish Research Council (VR Grant No 2017-04366, 2017-05962, 2020-00803) are acknowledged for financial support. We would like to thank Dalsjöfors Kött AB, Sweden, and their employees for their kind help with providing the adrenal glands.

Conflict of Interest

The authors declare no conflict of interest.

Data Availability Statement

The data that support the findings of this study are available from the corresponding author upon reasonable request.

Keywords: Amperometry · Chaotropic Effect · Hofmeister Series · Large Dense-Core Vesicles · Vesicle Opening

[1] R. C. Lin, R. H. Scheller, *Annu. Rev. Cell Dev. Biol.* **2000**, *16*, 19–49.
[2] R. D. Burgoyne, A. Morgan, *Physiol. Rev.* **2003**, *83*, 581–632.
[3] P. Thorn, R. Zorec, J. Retting, D. J. Keating, *J. Neurochem.* **2016**, *137*, 849–859.
[4] Q. Yue, X. Li, F. Wu, W. Ji, Y. Zhang, P. Yu, M. Zhang, W. Ma, M. Wang, L. Mao, *Angew. Chem. Int. Ed.* **2020**, *59*, 11061–11065; *Angew. Chem.* **2020**, *132*, 11154–11158.
[5] X. Kang, H. Xu, S. Teng, X. Zhang, Z. Deng, L. Zhou, P. Zuo, B. Liu, B. Liu, Q. Wu, L. Wang, M. Hu, H. Dou, W. Liu, F. Zhu, Q. Li, S. Guo, J. Gu, Q. Lei, J. Lü, Y. Mu, M. Jin, S. Wang, W. Jiang, K. Liu, C. Wang, W. Li, K. Zhang, Z. Zhou, *Proc. Natl. Acad. Sci. USA* **2014**, *111*, 15804–15809.
[6] A. J. B. Kreutzberger, V. Kiessling, C. A. Doyle, N. Schenk, C. M. Upchurch, M. Elmer-Dixon, A. E. Ward, J. Preobraschenski, S. S. Hussein, W. Tomaka, P. Seelheim, I. Kattan, M. Harris, B. Liang, A. K. Kenworthy, B. N. Desai, N. Leitinger, A. Anantharam, J. D. Castle, L. K. Tamm, *eLife* **2020**, *9*, e62506.
[7] P. C. Guest, *Adv. Exp. Med. Biol.* **2019**, *1134*, 17–32.
[8] A. Hatamie, L. Ren, H. Dou, N. R. Gandasi, P. Rorsman, A. Ewing, *Angew. Chem. Int. Ed.* **2021**, *60*, 7593–7596; *Angew. Chem.* **2021**, *133*, 7671–7674.
[9] M. Vakilian, Y. Tahamtani, K. Ghaedi, *Gene* **2019**, *706*, 52–61.
[10] Y. Wang, C. Gu, B. A. Patel, A. G. Ewing, *Angew. Chem. Int. Ed.* **2021**, *60*, 23552–23556; *Angew. Chem.* **2021**, *133*, 23744–23748.
[11] N. T. N. Phan, X. Li, A. G. Ewing, *Nat. Chem. Rev.* **2017**, *1*, 0048.
[12] E. Crivellato, B. Nico, D. Ribatti, *Anat. Rec.* **2008**, *291*, 1587–1602.
[13] T. Kim, M. C. Gondré-Lewis, I. Arnaoutova, Y. P. Loh, *Physiology* **2006**, *21*, 124–133.
[14] B. Coldren, R. van Zanten, M. J. Mackel, J. A. Zasadzinski, H. Jung, *Langmuir* **2003**, *19*, 5632–5639.
[15] J. Pencer, F. R. Hallett, *Langmuir* **2003**, *19*, 7488–7497.
[16] B. Vestad, A. Llorente, A. Neurauter, S. Phuyal, B. Kierulf, P. Kierulf, T. Skotland, K. Sandvig, K. B. F. Haug, R. Øvstebø, *J. Extracell. Vesicles* **2017**, *6*, 1344087.
[17] R. Pan, K. Hu, R. Jia, S. A. Rotenberg, D. Jiang, M. V. Mirkin, *J. Am. Chem. Soc.* **2020**, *142*, 5778–5784.
[18] R. Pan, K. Hu, D. Jiang, U. Samuni, M. V. Mirkin, *J. Am. Chem. Soc.* **2019**, *141*, 19555–19559.
[19] Y. Liu, C. Xu, P. Yu, X. Chen, J. Wang, L. Mao, *ChemElectroChem* **2018**, *5*, 2954–2962.
[20] X. Li, J. Dunevall, A. G. Ewing, *Acc. Chem. Res.* **2016**, *49*, 2347–2354.
[21] X. Li, J. Dunevall, L. Ren, A. G. Ewing, *Anal. Chem.* **2017**, *89*, 9416–9423.
[22] J. Dunevall, H. Fathali, N. Najafinobar, J. Lovric, J. Wigström, A.-S. Cans, A. G. Ewing, *J. Am. Chem. Soc.* **2015**, *137*, 4344–4346.
[23] X. Li, S. Majdi, J. Dunevall, H. Fathali, A. G. Ewing, *Angew. Chem. Int. Ed.* **2015**, *54*, 11978–11982; *Angew. Chem.* **2015**, *127*, 12146–12150.
[24] A. Thomen, N. Najafinobar, F. Penen, E. Kay, P. P. Upadhyay, X. Li, N. T. N. Phan, P. Malmberg, M. Klarqvist, S. Andersson, M. E. Kurczy, A. G. Ewing, *ACS Nano* **2020**, *14*, 4316–4325.
[25] J. Lovrić, J. Dunevall, A. Larsson, L. Ren, S. Andersson, A. Meibom, P. Malmberg, M. E. Kurczy, A. G. Ewing, *ACS Nano* **2017**, *11*, 3446–3455.
[26] K. Hu, R. Jia, A. Hatamie, K. Long Le Vo, M. V. Mirkin, A. G. Ewing, *J. Am. Chem. Soc.* **2020**, *142*, 16910–16914.

[27] X. Zhang, A. Hatamie, A. G. Ewing, *J. Am. Chem. Soc.* **2020**, *142*, 4093–4097.
[28] X. He, A. G. Ewing, *J. Am. Chem. Soc.* **2020**, *142*, 12591–12595.
[29] A. Oleinick, R. Hu, B. Ren, Z. Tian, I. Svir, C. Amatore, *J. Electrochem. Soc.* **2016**, *163*, H3014–H3024.
[30] C–T. Wang, R. Grishanin, C. A. Earles, P. Y. Chang, T. F. J. Martin, E. R. Chapman, M. B. Jackson, *Science* **2001**, *294*, 1111–1115.
[31] C. Amatore, S. Arbault, I. Bonifas, F. Lemaître, Y. Verchier, *ChemPhysChem* **2007**, *8*, 578–585.
[32] C. P. Grabner, S. D. Price, A. Lysakowski, A. P. Fox, *J. Neurophysiol.* **2005**, *94*, 2093–2104.
[33] J. C. Hutton, *Biochem. J.* **1982**, *204*, 171–178.
[34] L. Orci, M. Ravazzola, M. Amherdt, O. Madsen, A. Perrelet, J. D. Vassalli, R. G. Anderson, *J. Cell Biol.* **1986**, *103*, 2273–2281.
[35] S. Urbé, A. S. Dittie, S. A. Tooze, *Biochem. J.* **1997**, *321*, 65–74.
[36] B. R. Hajratwala, *J. Pharm. Sci.* **1975**, *64*, 45–47.
[37] D. R. Thakker, C. Boehlert, K. L. Kirk, R. Antkowiak, C. R. Creveling, *J. Biol. Chem.* **1986**, *261*, 178–184.
[38] L. Taylor, K. L. Harper, D. T. O'Connor, *N. Engl. J. Med.* **2003**, *348*, 1134–1149.
[39] Z. Jiang, C. B. Lietz, S. Podvin, M. C. Yoon, T. Toneff, V. Hook, A. J. O'Donoghue, *ACS Chem. Neurosci.* **2021**, *12*, 2385–2398.
[40] M. Lee, N. G. Gubernator, D. Sulzer, D. Sames, *J. Am. Chem. Soc.* **2010**, *132*, 8828–8830.
[41] K. I. Assaf, W. M. Nau, *Angew. Chem. Int. Ed.* **2018**, *57*, 13968–13981; *Angew. Chem.* **2018**, *130*, 14164–14177.
[42] X. He, K. Zhang, Y. Liu, F. Wu, P. Yu, L. Mao, *Angew. Chem. Int. Ed.* **2018**, *57*, 4590–4593; *Angew. Chem.* **2018**, *130*, 4680–4683.
[43] H. I. Okur, J. Hladilková, K. B. Rembert, Y. Cho, J. Heyda, J. Dzubiella, P. S. Cremer, P. Jungwirth, *J. Phys. Chem. B* **2017**, *121*, 1997–2014.
[44] P. Lo Nostro, B. W. Ninham, *Chem. Rev.* **2012**, *112*, 2286–2322.
[45] B. Kang, H. Tang, Z. Zhao, S. Song, *ACS Omega* **2020**, *5*, 6229–6239.

Manuscript received: November 28, 2021
Accepted manuscript online: February 7, 2022
Version of record online: February 18, 2022